

Exchange bias effect in antiferromagnets containing ferromagnetic clusters

M. L. Pankratova, and A. S. Kovalev

Citation: [Low Temperature Physics](#) **44**, 1161 (2018); doi: 10.1063/1.5060970

View online: <https://doi.org/10.1063/1.5060970>

View Table of Contents: <http://aip.scitation.org/toc/ltp/44/11>

Published by the [American Institute of Physics](#)

Articles you may be interested in

[In Honor of the 100th Anniversary of the National Academy of Sciences of Ukraine](#)

[Low Temperature Physics](#) **44**, 1111 (2018); 10.1063/1.5060962

[Phase diagram of the spin quantum Hall transition](#)

[Low Temperature Physics](#) **44**, 1219 (2018); 10.1063/1.5062164

[Electronic properties of graphene with point defects](#)

[Low Temperature Physics](#) **44**, 1112 (2018); 10.1063/1.5060964

[Experimental determination of the magnetic-field dependence of the low-temperature spontaneous magnetization of the electron system of hybridized states of cobalt impurities of low concentration \(\$\leq 0.035\$ at.%\) in a mercury selenide crystal](#)

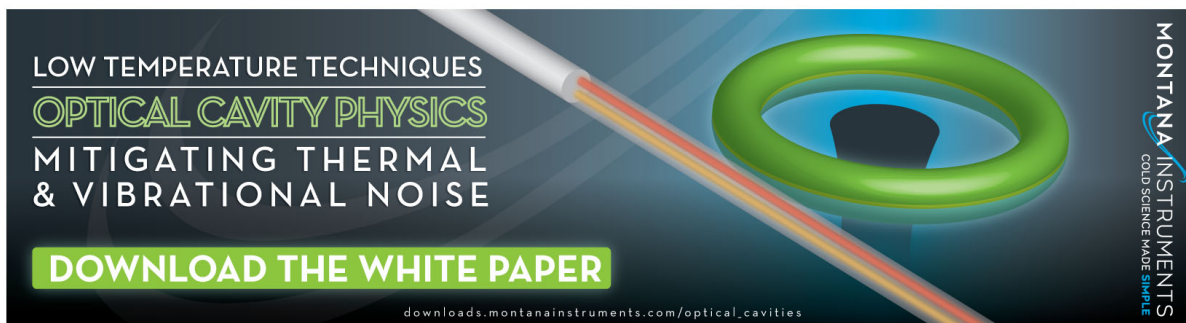
[Low Temperature Physics](#) **44**, 1221 (2018); 10.1063/1.5062165

[Features of magnetoresistance and magnetic properties in \$\text{Bi}_{0.569}\text{Mn}_{3.69}\text{Fe}_{0.62}\$](#)

[Low Temperature Physics](#) **44**, 1153 (2018); 10.1063/1.5060969

[Quantum quench for the biaxial spin system](#)

[Low Temperature Physics](#) **44**, 1173 (2018); 10.1063/1.5060972



LOW TEMPERATURE TECHNIQUES
OPTICAL CAVITY PHYSICS
MITIGATING THERMAL
& VIBRATIONAL NOISE

DOWNLOAD THE WHITE PAPER

downloads.montanainstruments.com/optical_cavities

MONTANA INSTRUMENTS
COLD SCIENCE MADE SIMPLE

The advertisement features a dark background with a glowing green ring and a fiber optic cable. The text is arranged in a clean, modern layout, with the main title in white and green, and the call to action in a green box. The Montana Instruments logo is positioned on the right side.

Exchange bias effect in antiferromagnets containing ferromagnetic clusters

M. L. Pankratova¹ and A. S. Kovalev^{2,3,a)}

¹Aston University, Birmingham, United Kingdom

²B. Verkin Institute for Low Temperature Physics and Engineering, National Academy of Sciences of Ukraine, 47 Nauki Ave., Kharkov, 61103, Ukraine

³V.N. Karazin Kharkiv National University, 4 Svobody Sq., Kharkov, 61022, Ukraine

(Submitted September 19, 2018)

Fiz. Nizk. Temp. **44**, 1485–1493 (November 2018)

This study offers an explanation for the occurrence of magnetization exchange bias in antiferromagnets with ferromagnetic inclusions during pre-cooling the system in a magnetic field. The ferromagnetic (FM) subsystem ordered in this field at the Néel temperature leads to an inhomogeneous state of the antiferromagnetic (AFM) matrix with the finite mean effective field at the FM/AFM interface. This field causes exchange bias in the dependence $M = M(H)$ during further remagnetization of the heterogeneous system. To describe the proposed scenario for such an effect, a simple model of a two-dimensional system with round inclusions of the FM phase was considered. Using numerical calculations and previously obtained analytical results, the study determines magnetization dependencies on the external field, which qualitatively explains the features of exchange bias in experimentally studied heterogeneous systems. *Published by AIP Publishing.*

<https://doi.org/10.1063/1.5060970>

1. Introduction

The phenomenon of ‘exchange bias’ (EB) is observed in inhomogeneous systems contacting ferromagnetic (FM) and antiferromagnetic (AFM) subsystems. It consists in the shift of the magnetization dependence of a magnet on the external magnetic field $M(\mathbf{H})$ from a symmetrical shape (relative to the field direction) by the value ΔH_{eb} . This effect was first observed in oxidized Co powder, i.e. ferromagnetic Co particles covered by a thin layer of antiferromagnetic CoO.¹ Subsequently, it was studied primarily using contacting FM/AFM films.^{2,3}

Exchange bias can be explained as follows.⁴ It is believed that, in an ideal homogeneous ferromagnet (FM), magnetic moments are collinearly aligned along an easy axis of magnetization. In an ideal homogeneous two-sublattice antiferromagnet (AFM), the moments of the sublattices are antiparallelly ordered in the same direction as in a ferromagnet. On certain sections of FM/AFM interfaces, AFM magnetic moments from one sublattice are present, i.e. they are collinearly ordered although they correspond to ideal antiferromagnetic ordering [see section *ab* in Figure 1 and *N* sections in Fig. 2(a)–(c)] (hereinafter ‘the uncompensated interface’). At the same time, they create an effective surface magnetic field (H_{eff}) acting on the FM subsystem in addition to the external field. In the case of other interface orientations [section *bc* in Fig. 1 and *C* sections in Fig. 2(a)–(c)], the effective surface magnetic field H_{eff} acting on the ferromagnet is cancelled out because these two have AFM magnetic moments from different sublattices (hereinafter ‘the compensated interface’). (Further, in order to be specific, it is assumed that the AFM subsystem is ordered in a chessboard arrangement.) An additional total field created by uncompensated interface sections determines the exchange bias of the H_{eb} field.

The exchange bias effect is determined by the interface between a ferromagnet and an antiferromagnet, the exchange

bias value being normally as follows: $\Delta H_{eb} \sim J_0 S/L$, where J_0 is the magnitude of the exchange interaction between the FM and AFM subsystems through the interface, S is the area of the uncompensated interface sections, and L is the characteristic size of the FM structure (FM clusters). Therefore, exchange bias is most prominently manifested in systems with a large interface surface, namely in contacting FM/AFM films with an uncompensated interface, or in a finely-dispersed heterogeneous medium with FM and AFM components. This primarily refers to multilayer systems made from thin FM and AFM films in which large surfaces of uncompensated interfaces can be created in the production process, and in which the volume of thin films is commensurate with the volume of boundaries. Such systems, manifesting the exchange bias effect, are successfully used in data recording and storage devices in which the surface of FM/AFM contacts is completely uncompensated and the effect manifests itself most strongly. However, the exchange bias effect was first observed in oxidized fine-grained cobalt powder with a large FM/AFM contact surface area, although in this system the average AFM magnetization at the interface must be zero. Therefore, despite a large number of both theoretical and experimental studies, this effect is yet to be thoroughly explained.^{4,5} Firstly, the problem is related to the complex structure of FM/AFM interfaces, which can include sections with ideal surfaces and compensated (with zero total magnetic moment) and uncompensated structures, as well as interface sections with differing degrees of roughness. Secondly, the exchange bias effect is significantly influenced by the conditions of sample production (cooling in an external magnetic field and the rate of this cooling).

One of the methods for studying these features of the exchange bias effect is the experimental study of heterogeneous FM/AFM systems, which are inclusions of FM clusters in an AFM matrix. This system is convenient because it has a large network of FM/AFM interfaces, i.e. it has a large

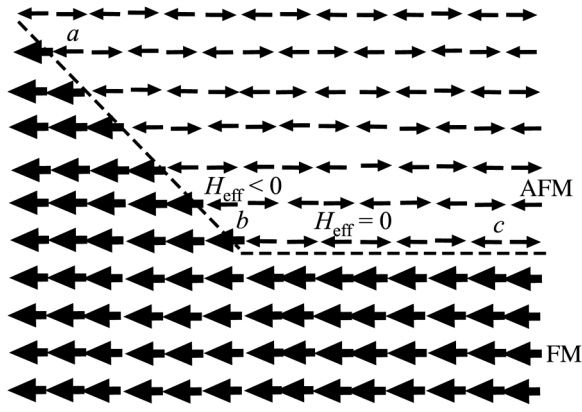


Fig. 1. Compensated (*bc*) and uncompensated (*ab*) interfaces between FM and AFM phases.

area (S) and is relatively small in size (L). Researchers study both metamaterials in which ferromagnetic elements form an ordered two-dimensional lattice on an AFM surface⁶ and disordered heterostructures in which FM clusters of different sizes and shapes are randomly incorporated into an AFM matrix.⁷⁻⁹ When cooled in an external magnetic field, a part of the system with ferromagnetic interparticle interaction transfers to a ferromagnetically ordered state. In the case of sufficiently large clusters, this can be associated with a cooperative phase transition in separate clusters, and at lower temperatures, it can be related to a bulk phase transition. In this case, the FM subsystem creates the mean field H_{eff} acting on the AFM matrix at its interface. The field acts within uncompensated interface sections, which serve as centres of nucleation of the AFM phase at the Néel temperature. However, in the case of a two-sublattice antiferromagnet, an increase in sections of the AFM phase from discrete FM clusters and from particular interface sections is accompanied by the formation of a system of AFM boundaries [Fig. 2(d)].

Recently, these heterogeneous systems have been intensively studied experimentally.⁷ In particular, they were

investigated in two studies^{8,9} that have reported observations of the exchange bias phenomenon. In this paper, we provide a model for the possible occurrence of exchange bias in heterogeneous FM/AFM systems. This model is investigated analytically and numerically using the results of theoretical studies^{10,11} of the field dependencies of planar FM/AFM interfaces.

The proposed scenario for the occurrence of exchange bias in heterogeneous systems can be described as follows. When a heterogeneous system is cooled in an external magnetic field H_{cool} , clusters with ferromagnetic interaction between magnetic moments pass into a magnetically ordered state with a non-zero average magnetization of the FM subsystem in the direction of the field. Given the finite size of the clusters, we are referring to the so-called ‘cooperative transition’, which is not accompanied by field dependence. At the same time, the ordered ferromagnet does not affect the AFM ordering on compensated interface sections (*bc* in Fig. 1). On uncompensated interface sections (*ab* in Fig. 1), the ferromagnet affects one of the AFM sublattices through the effective field directed along the external field, seeking to order it. At temperature T_N , uncompensated interface sections act as centres of nucleation of the AFM phase.

However, due to the two-sublattice AFM structure, distinct interface sections order particular AFM sublattices, and some of the emerging sections of the AFM phase do not connect with each other [see Fig. 2(d)], forming AFM domain boundaries (DB).

With a further decrease in temperature, the magnetic structure of the entire magnet is fixed and remains unchanged when the field is turned off. In particular, the AFM domain structure and the nature of AFM ordering at the boundaries with the FM are fixed. In this case, it is the AFM that affects FM clusters, which results in the effective field H_{eff} occurring on the uncompensated sections (*ab* in Fig. 1) and acting on the FM. This field is absent on the compensated sections (*bc* in Fig. 1). It is important that the total effective field acting on the surface of FM clusters on the part of the AFM

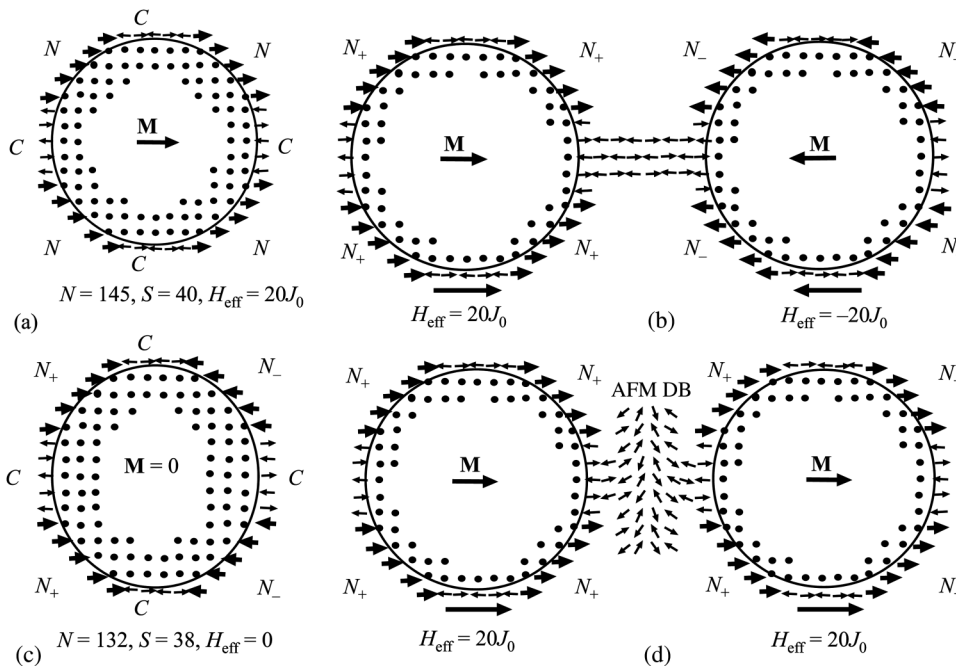


Fig. 2. AFM matrix ordering at the boundary with FM-ordered clusters (a), (c) and in areas between FM clusters (b), (d).

subsystem throughout the entire sample is non-zero. With further inclusion of a weak external field (smaller than the spin-flop field) and with further change in its orientation, the AFM system remains ‘frozen’ and the FM subsystem changes its magnetization direction. In this process, an important role is played by the ‘reverse’ effect of the H_{eff} field on FM clusters through uncompensated boundaries from the AFM. It acts as a field that is complementary to the external field and causes exchange bias.

2. Model

Let us consider a model of an FM cluster in an AFM matrix at low temperatures when both FM and AFM subsystems are magnetically ordered. To qualitatively describe this phenomenon and provide a clearer picture of remagnetization, we shall use a two-dimensional (2D) model of an AFM matrix and FM cluster (three-dimensional models are considered in Ref. 12). Cluster sizes and shapes are an extremely complicated issue because such sizes vary in experimental studies from 10 to 10^5 Å.¹³ At the same time, some studies consider metamaterials of 2D lattices of magnetic clusters with fixed sizes and shapes.⁶ Therefore, Sections 2 and 3, respectively, deal with large symmetrical clusters and small clusters of complex configuration. Moreover, we shall assume that an AFM matrix is an antiferromagnet whose magnetic moments are arranged in chessboard order [Fig. 2(a)]. The dots in the figure indicate the positions of FM moments in a cluster, and the fat arrows represent ‘frozen’ magnetic moments of the AFM matrix adjacent to the interface with an FM cluster.

The position of the cluster is selected so that its AFM environment in the ordered AFM state induces the maximum effective field $H_{\text{eff}} = 20J_0M_0$ on the cluster surface and causes its ordering in the direction of the vector \mathbf{M} .

On the other hand, in the presence of a cooling field that causes the ordering of the cluster in the \mathbf{M} direction, the cluster at the Néel transition also induces an effective field (H_{eff}) at the boundary, which results in ordering of the AFM matrix in its vicinity, as indicated in the figure. It is assumed that the symmetry of magnetic anisotropy and the size of a unit cell in the FM subsystem coincide with those in the AFM. This corresponds to the experimental situation in a number of studies^{7–9,13} that consider systems in which different magnetic subsystems have the same crystallographic structure but different charge states, which leads to ferro- and antiferromagnetic ordering. In addition, we assume that the external field is directed along the magnetic anisotropy axis common to the FM and AFM, and the field is smaller than the field of spin-flop transition in the AFM. In the case of a magnetically rigid AFM, the directions of the magnetic moments of the AFM are fixed, and FM moments can change orientation. For simplicity and clarity, let us also assume that, in the system, there is strong planar magnetic anisotropy which ‘places’ magnetic moments in a plane where they rotate.

Fig. 2(a) shows an FM cluster with 145 moments oriented along the axis of easy magnetization. In this case, the cluster radius R is $6a$, where a is the interatomic distance. It is shown below that, once a cluster has this radius, a further increase in its size has little effect on remagnetization. It can

be seen that for the selected location of the cluster centre, sections of compensated (C) and uncompensated (N) boundaries alternate at the interface. In this case, the effective fields of all uncompensated sections have one direction and the total uncompensated effective field is maximal.

However, if the same cluster is shifted in the AFM matrix by an odd number of interatomic distances (in the fixed ordering of the AFM matrix!), then the total effective field acting through the boundary on the FM core of the cluster will change its sign [the cluster on the right in Fig. 2(b)]. In the cluster configuration shown in Fig. 2(b), the total effective field acting on two clusters on the part of the AFM equals to zero, and, in the magnetic field at $T < T_N$, the total magnetization of the clusters will be zero without freezing. It should be noted that, in this case the entire AFM space outside these clusters can be ideally ordered without the emergence of domain boundaries. In addition, the total mean effective field acting on a cluster depends both on its shape and size.

For example, Fig. 2(c) shows a cluster similar to that shown in Fig. 2(a), although it is ‘flattened’ by one interatomic distance and contains 132 FM moments.

For this cluster, the total effective field associated with the ordered AFM matrix equals zero. In this figure, N_- and N_+ denote uncompensated sections with the opposite direction of the effective field. If the size of the cluster remains the same, it is possible to obtain the total effective field through the cluster interface in the interval $-H^* < H_{\text{eff}} < H^*$ (where $H^* \sim (2\pi R/a)J_{0M}/2$) by slightly varying the cluster’s shape and position in the AFM matrix in the perfect fixed alternation of AFM moments. Thus, in the absence of an external magnetic field during cooling, the mean effective field acting on the FM subsystem on the part of the AFM should be zero. In this case, the exchange bias effect is not observed, which was demonstrated experimentally in.^{8,9}

However, the situation can change as a result of the AFM passing into an ordered state when FM clusters have average magnetization oriented in one direction and caused by previous cooling in an external magnetic field. As indicated in the Introduction, ferromagnets have an ordering effect on antiferromagnets, and N sections at cluster boundaries act as nuclei of the AFM phase. In particular, with the same magnetization of the clusters in Fig. 2(d), the magnetic moments of the AFM subsystem on the N sections of the interface of the right cluster [see Fig. 2(d)] will be oriented in the direction of FM magnetization, i.e. in the direction opposite to that shown in Fig. 2(b). When the sample is further demagnetised, the external field acts weakly on the AFM subsystem, but the AFM’s remaining mean field results in the occurrence of magnetization exchange bias in FM clusters. However, it is apparent that, in such a scenario, AFM domain boundaries (like those shown in Fig. 2(d) between two clusters) are certain to arise, and some of the domain boundaries can ‘begin’ and ‘end’ at cluster boundaries. The additional energy of the system is associated with the emerging domain walls, and this energy must compete with the energy of an ordering mismatch between the FM and the AFM on N -type sections of interfaces in the absence of AFM boundaries. The number of AFM domain boundaries depends on the system’s cooling rate at the Néel phase transition. The resulting exchange bias should increase with an increase in the cooling rate.

3. Remagnetization of large radially symmetric clusters

Let us qualitatively consider remagnetization of a large-sized FM-ordered cluster in a magnetically ordered AFM matrix. In Ref. 12, this process was considered numerically using the mean field method and the Monte Carlo method for three-dimensional FM particles of spherical shape. The calculations showed that with a change in the external field in an FM cluster, the FM clusters contain areas of the phase ferromagnetically ordered along the field [N_- regions in Figs. 3(a) and 3(b)], which emerge from the ‘uncompensated’ sections of FM/AFM interfaces oriented against the field.

In the case of large-radius clusters ($R \gg a$), the inner areas of a ferromagnetic cluster can be qualitatively represented as alternating FM bands in contact with the boundaries ($N_+ - N_C - N_- - N_C$) of uncompensated sections oriented along (N_+) and against (N_-) the field, and of compensated sections (N_C), with the length deep into the cluster ($L \sim R$), and with a width of $\Delta \sim \pi R/4$. On these sections, the magnetization is approximately uniform along the width of the bands and varies only in the direction of the cluster centre [Fig. 3(b)]. In this figure, the lengths of the transition ordering regions along the field in the compensated and uncompensated regions are denoted as L_C and L_N . They are essentially different: $L_C \ll L_N$.

In the case of large-sized FM clusters, regions in contact with compensated and uncompensated AFM boundaries are rather wide. Therefore, for simplicity, we do not take into account the interaction between these regions, as we consider their contribution to the overall magnetization of a cluster as additive and understand the magnetization therein to be homogeneous along the width of the layer. In this case, the problem reduces to calculating the field dependencies of magnetization of individual FM regions that come into contact with various AFM boundaries, as is shown in Figure 3(b). This one-dimensional problem was previously investigated with respect to layered FM/AFM systems for uncompensated interfaces in Refs. 10 and 11 and for compensated and disordered boundaries in Refs. 14 and 15

This issue was considered theoretically in Refs. 10 and 11 with respect to FM films of finite thickness $L = aN$, where N is the number of FM atomic layers. A classical two-dimensional Heisenberg model was used for an easy-plane ferromagnet with additional weak anisotropy within the ‘easy plane’. A number of studies^{7–9} describe experiments on compounds in which manganese ions with spin $S = 2$ acted as

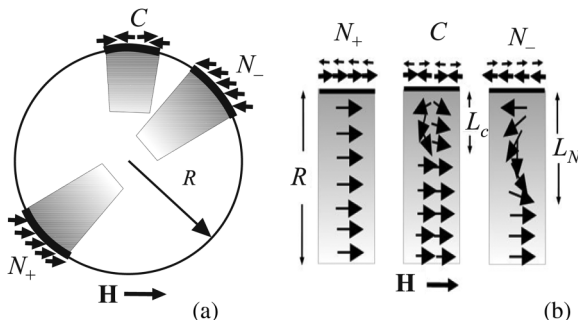


Fig. 3. Distribution of magnetization in FM cluster regions that are in contact with compensated (C) and uncompensated (N_{\pm}) boundaries at the interface.

magnetic moments, which justifies the classical description of the system. It was assumed that the main anisotropy was sufficiently large, the magnetization vectors did not come out of the easy plane and were characterized by only one scalar value, namely the angle of deviation φ from a favourable direction in the easy plane (the easy axis of magnetization). Since in regions with a compensated boundary (N_C) there are lines with different moment directions, which alternate along this boundary, the total energy in these regions, as calculated for the structure period along the boundary, can be written as follows:

$$E_C = - \sum_{i=1}^N \left(\sum_{j=1,2} \left(J \cos(\varphi_i^{(j)} - \varphi_{i+1}^{(j)}) + \frac{\beta}{2} \cos^2 \varphi_i^{(j)} + H \cos \varphi_i^{(j)} \right) + J \cos(\varphi_i^{(1)} - \varphi_i^{(2)}) \right) - \sum_{j=1,2} J_0 \cos(\varphi_1^{(j)} - \psi^{(j)}), \quad (1)$$

where J is the exchange interaction constant in the FM cluster, J_0 is the exchange constant across the FM/AFM interface, β is the single-ion magnetic anisotropy constant in the easy plane (the easy direction of magnetization in the FM and AFM is assumed to be the same and to coincide with the direction of the external magnetic field H). AFM magnetization is assumed to be fixed, i.e. the directions of magnetic moments in two AFM sublattices at the interface are characterized by the angles $\psi^{(1)} = 0$ and $\psi^{(2)} = \pi$.

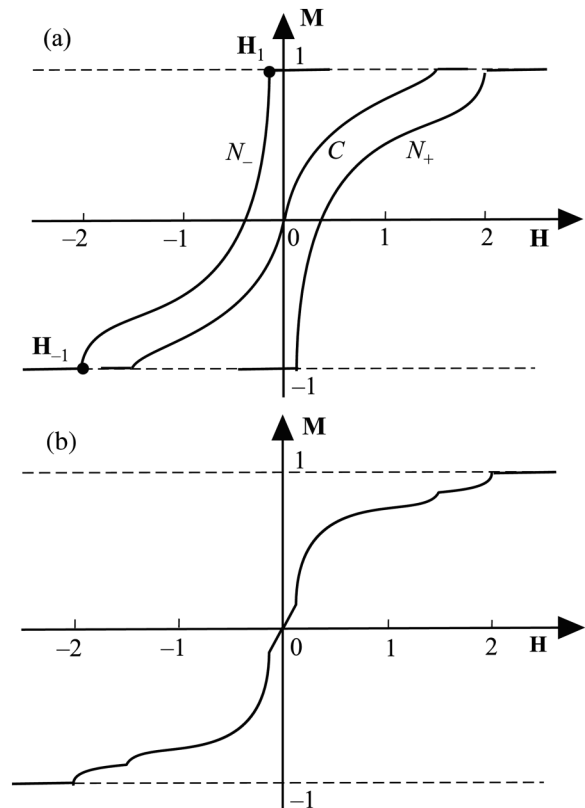


Fig. 4. Field dependencies of magnetization of FM regions with compensated and uncompensated boundaries of different signs (a) and the average dependence $M(H)$ for a system with the zero mean effective field of the AFM subsystem (b), i.e. where $C = 1/2$.

In regions with uncompensated boundaries (N_+) and (N_-), we assume that $\psi^{(j)}=0$ and $\psi^{(j)}=\pi$ respectively, and the energies as calculated for two layers perpendicular to the interface, are as follows:

$$E_{N_{\pm}} = -2 \sum_{i=1}^{N_{\pm}} \left(j \cos(\varphi_1^{(j)} - \varphi_{i+1}^{(j)}) + \frac{\beta}{2} \cos^2 \varphi_i^{(j)} + H \cos \varphi_i \right) \pm 2J_0 \cos \varphi_i, \quad (2)$$

Possible stable states of magnetization $\varphi_i^{(j)}(H)$ are determined by solving the equations $\partial E / \partial \varphi_i^{(j)} = 0$ and define the total magnetization of the system: $M(H) = \int_{i=1}^N (\cos \varphi_i^{(1)}(H) + \cos \varphi_i^{(2)}(H))$. The analytical dependencies of magnetization ($M(H)$) as a function of the parameters of the model J , J_0 and β are discussed in detail in Refs. 10 and 11.

First of all, let us consider the simple case of absence of magnetic anisotropy in FM clusters. For illustration, we present the field dependencies of magnetization (obtained numerically using the relaxation algorithm) for an isotropic FM with $\beta=0$ and with the ratio of exchange constants $J_0/J=2.7$ for the case $N=4$, which is somewhat smaller than the cluster sizes shown in Fig. 2. The magnetization M/J normalized to unity as a function of the field H/J (hereinafter $M=M(H)$) for different FM cluster regions (N_+ , C , N_-) is shown in Fig. 4(a). The dependencies $M=M(H)$ for

uncompensated sections (N_{\pm}) are similar to those obtained analytically in Ref. 16 using long wave approximation. If a sample is cooled in the absence of a field, then the sample average number of N_+ and N_- regions is equal and is half the number of regions with a compensated boundary. In this case, the field dependence of magnetization is symmetrical with respect to the direction of the field and there is no exchange bias. The complete (normalized) dependence $M(H)$ is as follows: $M(H) = (2M_C + M_{N_+} + M_{N_-})/4$. It is presented for the particular case of the cluster shown in Fig. 4(b).

If a heterogeneous FM/AFM system is cooled in a field, the concentration of sections of uncompensated boundaries with different directions of magnetization in FM clusters becomes different and is determined by the direction and magnitude of the external field, the total average field dependence of magnetization to be described by the following formula:

$$M(H) = (M_C + (1 - C)M_{N_+} + CM_{N_-})/4. \quad (3)$$

For example, this dependence is shown in Fig. 5(a) in respect of the concentration $C=1/4$ for which the areas of surfaces oriented along and against the field differ by a factor of three. The figure shows the occurrence of exchange bias of a magnetization curve. However, since critical field values do not change, exchange bias does not reduce simply to a shift of the entire previously symmetrical curve along the value axis of fields. The magnetization curve deforms significantly and the asymmetry of the field dependence $M(H)$ arises. Apart from the exchange bias of the curve along the field, there is also additional bias in magnetization magnitude. This was noted when discussing the results of experiments in Ref. 9.

Fig. 5(b) shows similar curves for different C concentrations over the range $0 < C < 1$ as determined by the magnitude of the external field in cooling samples and by the rate of such cooling.

In this figure, we can see only some of the dependencies for one field direction ($H < 0$). The full picture of field dependencies can be obtained as follows: $H \rightarrow -H$, $M \rightarrow -M$ and $C \rightarrow 1 - C$. In the field region $H_1 < H < 0$, magnetization curves are characterized by a parallel shift along the M axis, proportional to concentration C .

The results obtained allow us to plot the dependencies of exchange bias magnitude on the effective impact of the AFM subsystem on FM clusters, which provides some insight into the influence of cooling field magnitude and cooling rate on the magnetic structure of a cluster surface. This issue was discussed earlier in Ref. 9: the boundary line in Fig. 5(b) for concentrations $C=0$ corresponds with the line $M_C(H)$ in Fig. 4(a). The $M(H)$ dependencies shown in Fig. 5(b) allow us to find a relationship between the magnitude of exchange bias and the characteristic of the magnetic structure of a cluster surface, i.e. the concentration of various uncompensated sections. In this case, it is necessary to use the typical exchange bias of a magnetization curve along the field $\Delta H_{eb} = \Delta H_{eb}(C)$ and over magnetization magnitude in a zero external field $\Delta E_{eb} = \Delta E_{eb}(C)$.

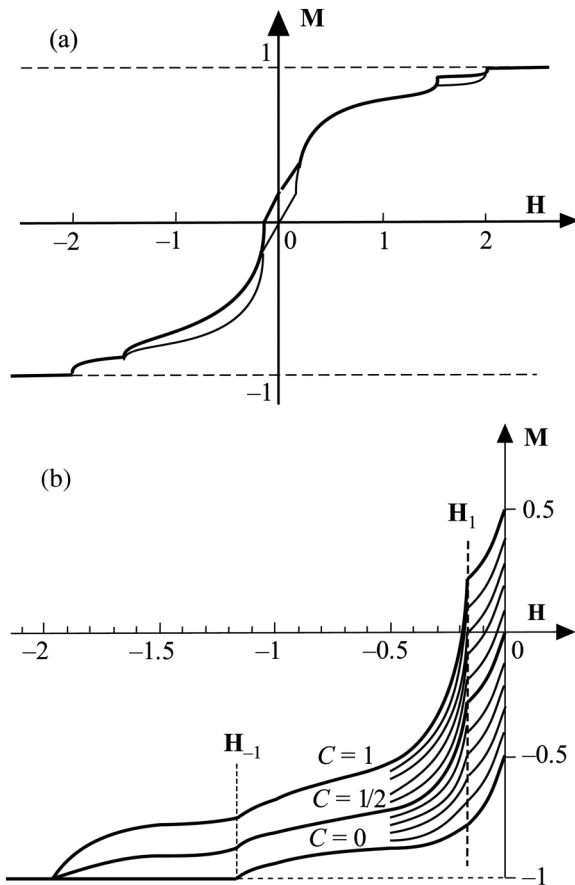


Fig. 5. Field dependence of magnetization of a heterogeneous FM/AFM system with the concentration of uncompensated boundaries $C=1/4$ (bold curve) and the dependence from Fig. 4(b) for the concentration $C=1/2$ (a) (thin line). Analogous field dependencies for different concentrations over the range $0 < C < 1$. Thick lines correspond to concentrations $C=0.1/2.1$ (b).

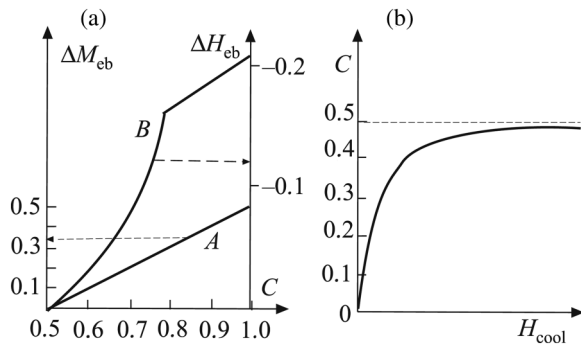


Fig. 6. Dependence of the exchange bias of magnetization (A) and a field (B) on the concentration of the uncompensated section of the interface (effective bias field) (a). Qualitative dependence of the concentration C of uncompensated sections of cluster boundaries on the cooling field (b).

This magnitude is strictly linear in terms of concentration and is shown in Fig. 6(a) as straight line A. Bias field dependencies are slightly different from the magnetization bias [line B in Fig. 6(a)]. In the field region $H_1 < H < 0$, it replicates the field dependence of magnetization at a fixed concentration, and at high concentrations, it is almost linear. Therefore, using the experimental results for exchange bias as a function of the cooling field H_{cool} as obtained in Ref. 9 [Fig. 5(a) in Ref. 9], we can plot the dependence of concentration C and the effective field H_{eff} on the field H_{cool} . It is shown qualitatively in Fig. 6(b).

Figures 4–6 present the results of calculations for clusters whose characteristic size (cluster radius or the length of the region in contact with a homogeneous section of the boundary) is chosen equal to $N=4$.

The figures clearly show all the features of the magnetization curves and their shifts depending on the values of the external field and magnetization.

4. Influence of cluster sizes and magnetic anisotropy on the nature of the remagnetization of a heterogeneous system

Let us discuss the effect of cluster size on the exchange bias effect if the cluster radius is sufficiently large. Figs. 7(a) and 7(b) show how the form of the field dependencies of magnetization in regions with compensated and uncompensated C and N_- boundaries (shown in Fig. 3(a) for $N=4$)

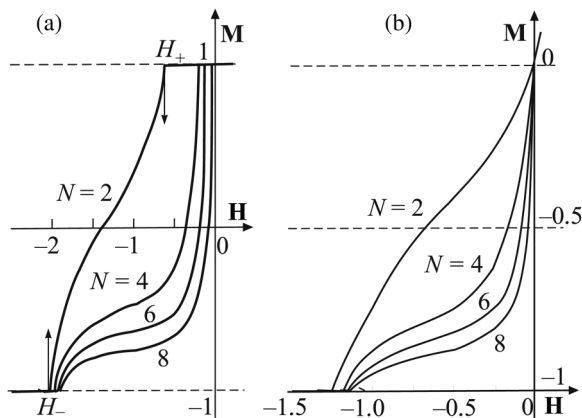


Fig. 7. Field dependencies of magnetization of FM sections bordering the uncompensated (a) and compensated (b) sections of the FM/AFM boundary for different values of size N .

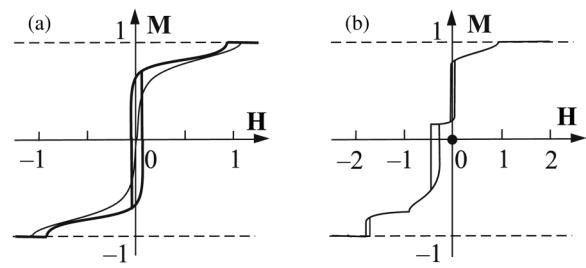


Fig. 8. Field dependencies of an FM region with a compensated boundary with an AFM taking into account anisotropy (bold curve) and in the case of an isotropic easy plane (thin curve) (a). The same applies for the case of equal concentrations of compensated sections (C) and uncompensated sections (N_+), i.e. where $C=0$ (b).

changes with a change in cluster size. Contained here are results obtained for $1 \leq N \leq 8$. It can be seen that, with an increase in cluster size, the magnitude of exchange bias decreases. This is consistent with the results obtained in Ref. 10 in the long-wavelength limit for FM films bordering the AFM system:

$$\begin{aligned} \sqrt{H_+/J} \operatorname{tg}\left(N\sqrt{H_+/J}\right) &= (J_0/J), \\ \sqrt{H_-/J} \operatorname{th}\left(N\sqrt{H_-/J}\right) &= (J_0/J). \end{aligned} \quad (4)$$

In the case of the H_+ field boundary, there is good quantitative agreement between the analytical and numerical results: $H_+/J \approx (\pi/2N)^2$. For the H_- boundary, the agreement is of a qualitative nature, which is associated with the effect of lattice discreteness. ‘Shelves’ in the dependencies of magnetization on the field for the selected parameters correspond to a revolution of magnetization in a layer of the order of one interatomic distance (the result of considering a discrete model). Therefore, in the normalized variables $M = M_{\text{tot}}/\pi R^2 a$, it decreases and is on the order of $1/N$. Qualitatively, however, the $M(H)$ dependencies have the same form as shown in Fig. 4.

Finally, let us discuss the effect of weak anisotropy in the magnetic easy plane ($\beta \neq 0$) on the magnetic characteristics of clusters (see Ref. 16). Fig. 8(a) shows the field dependencies of magnetization of an FM region in contact with a compensated AFM boundary in the case $N=4$, $J_0/J=2.7$ in the presence of anisotropy, $\beta/J=0.25$ (thick line), and in the absence of this additional anisotropy (thin curve). Anisotropy leads to hysteresis in field dependence; however, these dependencies coincide quite well, both qualitatively and quantitatively.

Figure 8(b) shows the dependence of magnetization in a system with equal concentrations of sections of compensated and uncompensated interphase boundaries ($J_0/J=2.7$, $\beta/J=0.25$, $N=4$, and $C=0$). Its comparison with the dependence in Figure 4 for the system without taking into account anisotropy ($C=1/4$) reveals that the presence of weak anisotropy does not qualitatively change the nature of field dependence and its bias, but results in the occurrence of narrow hysteresis loops.

5. Conclusion

Thus, this paper proposes a scenario for the occurrence of exchange bias in heterogeneous systems, which are an

ensemble of FM clusters in an AFM matrix. When a system is cooled in an external magnetic field, FM ordering arises in clusters. With a further decrease in temperature in the Néel transition region, this leads to an ordering of the AFM subsystem, which results in an effective field occurring at FM/AFM interfaces and action upon the FM via the AFM through uncompensated interfaces. This field is associated with the domainization of the antiferromagnet, which persists after the external field is turned off. With further application of a differently directed weak external field, the exchange bias is determined by the combined influence of external and effective fields.

To describe the proposed scenario, the authors consider a simple model of a two-dimensional system with round inclusions of the FM phase. Using previously obtained analytical results and numerical calculations, we have established the dependencies of magnetization on the external field for small clusters, which qualitatively explain the features of exchange bias in heterogeneous systems. Emphasis is placed on the differing type of exchange bias in relation to the magnitude of the field and the magnitude of magnetization. Experimental data obtained for exchange bias in heterogeneous systems are also discussed.

This individual study has been supported as part of Research Project No. 4.17 N (funded by the National Academy of Sciences of Ukraine) and Research Programme 1.4.10.26/F264. It has also been supported by the TUMOCS project. The project is funded by the European Commission under Horizon 2020's Marie Skłodowska-Curie Actions scheme (Grant No. 645660).

^{a)}Email: kovalev@ilt.kharkov.ua

¹W. H. Maklejohn and C. P. Bean, *Phys. Rev.* **102**, 1413 (1956).

²J. Nogues and I. K. Schuller, *J. Magn. Magn. Mater.* **192**, 203 (1999).

³A. E. Berkowitz and K. Takano, *J. Magn. Magn. Mater.* **200**, 552 (1999).

⁴M. Kiwi, *J. Magn. Magn. Mater.* **234**, 584 (2001).

⁵M. Pankratova, A. Kovalev, and M. Žukovič, *Understanding of Exchange Bias in Ferromagnetic/Antiferromagnetic Bilayers*, in: *Exchange Bias: From Thin Film to Nanogranular and Bulk Systems*, CRC PRESS-TAYLOR & FRANCIS GROUP (2205).

⁶S. Laureti, S. Y. Suck, H. Haas, E. Prestat, O. Bourgeois, and D. Givord, *Phys. Rev. Lett.* **108**, 077205 (2012).

⁷D. Niebieskikwiat and M. B. Salamon, *Phys. Rev. B* **72**, 174422 (2005).

⁸E. L. Fertman, S. Dolya, V. Desnenko, L.A. Pozhar, M. Kajnakova, and A. Feher, *J. Appl. Phys.* **115**, 203906 (2014).

⁹E. L. Fertman, A. V. Fedorchenko, O. V. Kotlyar, V.O. Desnenko, E. Čižmár, A. Baran, D.D. Khalyavin, A.N. Salak, V.V. Shvartsman, and A. Feher, *Fiz. Nizk. Temp.* **41**, 1001 (2015) [*Low Temp. Phys.* **41**, 724 (2015)].

¹⁰A. G. Grechnev, A. S. Kovalev, and M. L. Pankratova, *Fiz. Nizk. Temp.* **38**, 1184 (2012) [*Low Temp. Phys.* **38**, 937 (2012)].

¹¹A. G. Grechnev, A. S. Kovalev, M. L. Pankratova, *Fiz. Nizk. Temp.* **39**, 1361 (2013) [*Low Temp. Phys.* **39**, 1060 (2013)].

¹²O. Iglesias, A. Labarta, and X. Batlle, *J. Nanoscience Nanotechnology* **8**, 2761 (2008).

¹³Xiao-Juan Fan, H. Koinuma, and T. Hasegawa, *Phys. Rev. B* **65**, 144401 (2002).

¹⁴A. Kovalev and M. Pankratova, *Superlattices and Micro-structures* **73**, 275 (2014).

¹⁵A. S. Kovalev, M. L. Pankratova, *Fiz. Nizk. Temp.* **40**, 1267 (2014) [*Low Temp. Phys.* **40**, 990 (2014)].

¹⁶A. G. Grechnev, A. S. Kovalev, and M. L. Pankratova, *Fiz. Nizk. Temp.* **35**, 670 (2009) [*Low Temp. Phys.* **35**, 526, (2009)].

Translated by CWS